

11-27-2020

## Theoretical Model to Predict the Performance of Centrifugal Pump Equipped with Splitter Blades.

Berge Djebedjian

*Professor of Mechanical Power Engineering Department, Faculty of Engineering, Mansoura University, El-Mansoura 35516, Egypt, bergedje@mans.edu.eg*

Follow this and additional works at: <https://mej.researchcommons.org/home>

---

### Recommended Citation

Djebedjian, Berge (2020) "Theoretical Model to Predict the Performance of Centrifugal Pump Equipped with Splitter Blades.," *Mansoura Engineering Journal*: Vol. 34 : Iss. 2 , Article 26.

Available at: <https://doi.org/10.21608/bfemu.2020.126166>

This Original Study is brought to you for free and open access by Mansoura Engineering Journal. It has been accepted for inclusion in Mansoura Engineering Journal by an authorized editor of Mansoura Engineering Journal. For more information, please contact [mej@mans.edu.eg](mailto:mej@mans.edu.eg).

# THEORETICAL MODEL TO PREDICT THE PERFORMANCE OF CENTRIFUGAL PUMP EQUIPPED WITH SPLITTER BLADES

Berge Djebedjian

Mechanical Power Engineering Department, Faculty of Engineering,  
Mansoura University, El-Mansoura, Egypt  
E-Mail: bergedje@mans.edu.eg

نموذج نظري للتنبؤ بأداء المضخة الطاردة المركزية المجهزة بريش فاصلة

## الخلاصة:

تقدم هذه الدراسة نتائج النموذج النظري للتنبؤ بأداء مضخة لها دفاعة طاردة مركزية مجهزة بريش فاصلة. المنهجية المقترحة تأخذ الاختلافات التصميمية لمضخة مزودة بريش فاصلة بالمقارنة مع المضخة التقليدية. في حالة التدفق خلال حلقات من الريش المحورية، هناك تأثيراً متميزاً للصلابة على زاوية خروج التدفق من الريش. استخدم هذا التشابه في اشتقاق معامل الانزلاق للدفاعات المجهزة بريش فاصلة. تم إجراء تحليل الفوائد للتنبؤ بأداء مضخات الطرد المركزي ومقارنة النتائج النظرية مع النتائج التجريبية المتاحة. أوضحت القيم النظرية للسمت مع تغير معدل تدفق المضخة وجود اتفاق معقول مع القياسات.

## ABSTRACT

This study presents the results of the theoretical model to predict the centrifugal pump performance when its impeller is equipped with splitters. The proposed methodology accounts for the constructional differences of the pump equipped with splitter blades as compared with the conventional pump. For flow through axial blade rings, there is a distinct influence of the solidity on the outflow angle from the blades. This analogy is used for the derivation of a slip factor for impellers with splitters. A loss analysis procedure has been presented to predict the performance of centrifugal pumps. The result is compared with available experimental results. The predicted values of head over the operating range of flow rate of the pump have been found to be in reasonable agreement with the measurements.

**Keywords:** Centrifugal Pumps, Performance, Slip Factor, Losses

## NOMENCLATURE

$b$	impeller width	$C_u$	ideal whirl velocity
$C$	absolute velocity	$C_u'$	actual whirl velocity
$C_3$	velocity approaching volute throat	$D_3$	mean inlet diameter of volute throat
$C_d$	dissipation coefficient	$D_h$	hydraulic diameter for flow passage
$C_f$	friction coefficient	$f$	friction factor
$C_{fr}$	disk friction coefficient	$g$	gravitational acceleration
$C_{Q3}$	velocity at the throat	$h$	head loss due to flow phenomena
$C_r$	radial velocity	$H$	head
		$H_m$	manometric head
		$k_s$	disk surface roughness

$L$	length
$M_{DF}$	frictional torque of disk
$N$	pump speed
$P_e$	input power
$P_{DF}$	disk friction power
$Q$	pump flow rate
$R$	impeller radius
$Re$	Reynolds number
$s$	axial gap between disk and housing
$t$	blade thickness
$U$	impeller peripheral velocity
$W$	relative velocity
$Z$	number of blades in the impeller
$\alpha$	flow angle
$\beta$	blade angle
$\gamma$	specific gravity of water
$\varepsilon$	roughness height
$\varepsilon_{\text{limit}}$	limiting radius ratio
$\eta$	overall efficiency
$\nu$	kinematic viscosity of water
$\rho$	density of water
$\sigma$	solidity
$\sigma_s$	slip factor
$\omega$	impeller angular velocity

**Subscripts**

1	impeller eye
2	impeller tip
$av$	average
$b$	blade
$c$	circulation
<i>Disk</i>	disk
$f$	friction
$i$	incidence
$l$	leakage
$s$	splitter
$th$	theoretical
$thn$	net theoretical
<i>Vol</i>	volute

**1. INTRODUCTION**

Centrifugal pumps are used in water distribution systems to overcome gravity and friction losses in pipes to move water. Low-specific-speed high-speed centrifugal pumps are widely used in petrochemical, aerospace and chemical industries to

deliver low flow rate and high-head liquids, but there exist many problems to be solved, such as low efficiency due to disc friction loss and low flow rate instability due to positive slope of head-capacity characteristic curve, Cui et al. [1]. Through the experimental study on the low-specific-speed high-speed centrifugal pumps, it is found that the impeller with splitter blades can effectively solve these problems, Zuchao et al. [2].

Splitter blades are blades positioned between main blades for additional flow control and for reducing main blade loading. The impellers with splitter blades between two long blades can be used to alleviate the serious clogging at the inlet of the impeller caused by more blades.

The studies concerned with the performance of centrifugal pumps equipped with splitter blades can be classified into three categories: (a) Experimental studies, (b) Numerical studies, and (c) Theoretical studies.

(a) **Experimental studies:** the measurements of inlet and outlet pressures and input power, and the calculation of pump efficiency were included.

Nakase and Senoo [3], in their numerical and experimental study, pointed out that the circumferential position of the splitter blades has some influence on the delivery head of the pump.

Khlopenkov [4] stated that to optimize the flow regimes, it is convenient to install in the zone of the increased vane inclination 1-5 additional short blades with a length amounting to 0.6-1.2 of the length of the swept-forward tips of the main blades.

Gui et al. [5] studied experimentally the effects of splitter blades on a forward-curved centrifugal fan performance. Their results show that the circumferential position and the stagger angle of the splitter blades have an obvious influence on the performance while properly lengthened splitter blades can raise the total pressure coefficient.

Miyamoto et al. [6] examined the

influence of the splitter blades on flow and performance by measuring velocity and pressure in the un-shrouded and shrouded impeller passages. The length of splitter blades was approximately 60% of the length of main blades. They pointed out that in impellers with splitter blades the blade loading tends to become smaller, and the absolute circumferential velocities and total pressures become considerably larger than those in impellers without splitter blades.

Yuan [7] revealed that the splitter blade technique is one of the techniques to solve three hydraulic problems of low-specific-speed centrifugal pumps (relatively lower efficiency, drooping head-flow curve, and easily overload brake horsepower characteristics). The radial length of the splitter blade was fixed to 70% of the main blade length or 50–75% of the impeller outlet diameter. He pointed out that the effects of splitter blades on pump performance depend on the primary circumferential position and then blade discharge angle. Other parameters include the inlet diameter and fixing situation. The splitter blade offset will prevent the flow from separating on the suction surface and improve the velocity distribution within an impeller. Hence, the hydraulic losses within an impeller and mixed losses from the impeller outlet to the casing inlet can be reduced, thus improving the pump performance.

Gölcü et al. [8-10] examined experimentally the effects of different lengths of splitter blades on the performance of the deep well pump. They concluded that increasing the number of blades increases the head of the pump; however, it causes a decrease in efficiency due to the blockage effect of the blade thickness and friction.

**(b) Numerical studies:** Computational Fluid Dynamics (CFD) in simulation of the flow field in centrifugal impeller was applied.

Cui et al. [1] simulated numerically the three-dimensional turbulent flow in four

low-specific-speed centrifugal impellers based on the Navier-Stokes equations and the Spalart-Allmaras turbulence model. The simulated results show that the complex impeller with long, mid and short blades can improve the velocity distribution and reduce the back flow in the impeller channel. The experimental results show that the back flow in the impeller has an important influence on the performance of pump and a more-blade complex impeller with long, mid and short blades can effectively solve low flow rate instability of the low-specific-speed centrifugal pump.

Kergourlay et al. [11] studied numerically the influence of adding splitter blades on the performance of a hydraulic centrifugal pump. Adding splitters has negative and positive effects on the pump behavior. It increases the head rise compared to the original impeller. But the efficiency is not improved since the hydrodynamic losses are greater. It decreases the pressure fluctuations and reorganizes more conveniently the flow at the volute outlet.

**(c) Theoretical studies:** the theoretical head of pump, the slip factor, and the losses in impeller, diffuser and volute were calculated to predict the pump performance characteristics.

Ukhin [12] estimated the theoretical characteristic  $H-Q$  for dredge pumps with splitter blades by calculating the constraint coefficient based on the final number of blades and the flow separation from the blades. The proposed method lacks the effect of splitter blade length.

Analytical calculations of pump characteristics depend on geometrical dimensions of pumps and loss models. The pump characteristic relationship  $H = f(Q)$  is not well-estimated because of the failure of calculation to include accurate loss factors in pumps. Although a series of formulae for calculating losses exist but they lack accuracy when applied to centrifugal pumps.

The determination of the pump

characteristics using quasi-empirical basis faces the difficulties of predicting accurate loss coefficients.

Tuzson [13] proposed a calculation procedure to estimate the theoretical performance of centrifugal pumps. He presented a simple and fast calculation procedure with minimal input requirements. Flow conditions are calculated on an average streamline through the pump.

Zaher [14] suggested an approximate method for calculating radial flow pump characteristics by treating the losses at different elements of the pump at a selected point of operation, as having a constant coefficient of loss. Values of losses were calculated from the actual pressure heads. The comparison between the predicted characteristics and measured data for several pump investigations presented good agreement in some cases.

The prediction models developed for conventional pumps are not applicable directly to pumps equipped with splitter blades. For example, the slip factor should be modified to estimate reasonable theoretical pump heads.

The phenomenon of slip is well known to strongly influence the performance of centrifugal pumps. The slip factor does not represent a hydraulic loss. It just stands for a reduction in the capability of the pump to transfer energy. The most representative attempts to estimate slip factors are mentioned. Busemann [15] obtained values of the slip factor by means of potential flow analysis. However, the flow within a centrifugal pump impeller near the walls is far from potential, and this analysis could result in faulty approximations. Pfleiderer [16] developed a method to calculate the slip assuming a uniform distribution of the pressure around the blade. Stodola [17] assumed a rotating cylinder of fluid at the end of the interblade channel as the cause of the slippage. Stanitz [18] proposed a slip factor correlation derived from the results of two-dimensional fluid flow solutions. Wiesner [19] carried out a comprehensive

review and concluded that the method of Busemann was still the most accurate. Furthermore, Wiesner [19] proposed a correlation fitting the Busemann data extremely well up to a limiting inlet-to-outlet impeller radius ratio beyond which an empirical correction factor was presented.

Von Backström [20] proposed a simple analytical method to derive the slip velocity in terms of a Single Relative Eddy (SRE). He tried to unify the other prediction methods. However, none of the proposed methods are general and they produce different results even when applied to the same impeller.

Memardefzouli and Nourbakhsh [21] observed that in the design-point condition of the pumps, the experimental values of the slip factor are in good agreement with the theoretical values. However, there are significant disagreements between the theoretical and experimental values at off-design regiments. The difference is more apparent at low flow rates. The slip factor is by no means a constant for a given impeller. In fact, it is constant around the design point but it decreases with decreasing flow rate.

In the present study, an attempt is made to develop an improved methodology to predict the performance of centrifugal pumps equipped with splitter blades by analyzing various losses in the pump. The procedure proposed by Tuzson [13] is followed to estimate the losses. A computer program is written to facilitate the estimation of the pump characteristics as a function of the pump dimensions. The predicted values show reasonable agreement with the measured values.

## 2. SLIP FACTOR

Basically, there are two definitions of slip factor [20]. Both are equal to one minus the normalized slip velocity. In the first definition, the slip velocity is normalized by the impeller tangential velocity  $\sigma_s = 1 - C_s/U_2$  and in the second

by the ideal whirl velocity  $\sigma_s = 1 - C_s/C_{u2}$ . The first definition is used in this study because of the difficulties of the dependency of  $C_{u2}$  on the flow through the impeller.

In spite of its highly empirical origin, Wiesner's correlation, [19], has maintained great acceptance among researchers aiming to predict the performance of centrifugal pumps, Gülich [22]. It is given as, Wiesner [19]:

$$\sigma_s = 1 - \frac{\sqrt{\sin \beta_2}}{Z^{0.7}} \quad \text{for } \frac{R_1}{R_2} \leq \varepsilon_{\text{limit}} \quad (1)$$

and

$$\sigma_s = \left( 1 - \frac{\sqrt{\sin \beta_2}}{Z^{0.7}} \right) \left[ 1 - \left( \frac{R_1/R_2 - \varepsilon_{\text{limit}}}{1 - \varepsilon_{\text{limit}}} \right)^3 \right] \quad \text{for } \frac{R_1}{R_2} > \varepsilon_{\text{limit}} \quad (2)$$

where  $\varepsilon_{\text{limit}}$  is the limiting radius ratio,

$$\varepsilon_{\text{limit}} = \exp\left(-\frac{8.16 \sin \beta_2}{Z}\right) \quad (3)$$

### 3. LOSS MODELS

The calculation of the performance of centrifugal pumps is based on the loss correlations. There are many empirical models for prediction of the losses. In the present study, the loss correlations for the following internal losses are taken into consideration: (a) Inlet incidence loss, (b) Impeller frictional head loss, (c) Diffusion loss, and (d) Volute head loss. Also, the following parasitic losses are considered: (a) Disc friction loss, (b) Inlet recirculation losses, and (c) Leakage loss.

The study is based upon the blockage created by putting the spoilers in the impeller. The blade thickness decreases the space available for passing the flow. Consequently, an increase in local velocities is the result which yields creation

of disturbances caused by the blade edges at leading and tail.

### 3.1 Theoretical Head

The Euler's head equation for an infinite number of blades is:

$$H_{th} = (U_2 C_{u2} - U_1 C_{u1})/g \quad (4)$$

where  $g$  is the acceleration of gravity,  $U_1$  and  $U_2$  are the tangential velocities at inlet and outlet, and  $C_{u1}$  and  $C_{u2}$  are the ideal whirl velocities at inlet and outlet, respectively, Fig. 1, given as:

$$U_1 = \pi D_1 N/60 \quad (5)$$

$$U_2 = \pi D_2 N/60 \quad (6)$$

$$C_{u1} = U_1 - C_{r1} \cot \beta_1 = U_1 - \frac{Q \cot \beta_1}{\pi D_1 b_1 - Z t b_1 / \sin \beta_1} \quad (7)$$

$$C_{u2} = U_2 - C_{r2} \cot \beta_2 = U_2 - \frac{Q \cot \beta_2}{\pi D_2 b_2 - Z t b_2 / \sin \beta_2} \quad \dots (8)$$

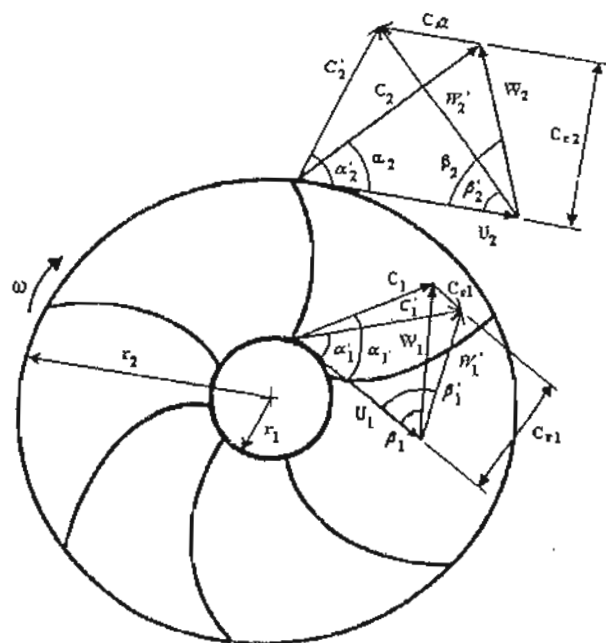


Fig. 1 Inlet and outlet velocity triangles without ( $C_1, W_1; C_2, W_2$ ) and with slip effect ( $C_1', W_1'; C_2', W_2'$ )

### 3.2 Net Theoretical Head

The net theoretical head is the head obtained using a finite number of blades. It is obtained using the actual whirl velocities:

$$H_{thn} = (U_2 C'_{u2} - U_1 C'_{u1}) / g \quad (9)$$

### 3.3 Circulation Head

The circulatory flow that results from the flow of a fluid inside a completely closed impeller channel when the impeller is rotating causes an increase in the relative velocity  $W$  at the suction surface of the blade and a decrease in  $W$  at the pressure surface of the blade by a slip velocity, Fig. 2. At the inlet and exit of impeller, the contribution of the slip velocity,  $C_s$ , is given by the slip factor,  $\sigma_s$ .

The circulation head due to channel circulation is given as:

$$\begin{aligned} H_c &= H_{th} - H_{thn} \\ &= [U_2 (C_{u2} - C'_{u2}) + U_1 (C'_{u1} - C_{u1})] / g \\ &= (U_2 C_{s2} + U_1 C_{s1}) / g \end{aligned} \quad (10)$$

The slip velocity at inlet,  $C_{s1}$ , is in the direction of the peripheral velocity,  $U_1$ , while the slip velocity at exit,  $C_{s2}$ , is in the opposite direction of the peripheral velocity,  $U_2$ . The slip velocities are given by:

$$C_{s1} = (1 - \sigma_{s1}) U_1 = C'_{u1} - C_{u1} \quad (11)$$

$$C_{s2} = (1 - \sigma_{s2}) U_2 = C_{u2} - C'_{u2} \quad (12)$$

From Eq. (11) and (12), the actual whirl velocities can be written as:

$$C'_{u1} = U_1 (2 - \sigma_{s1}) - C_{r1} \cot \beta_1 \quad (13)$$

$$C'_{u2} = U_2 \sigma_{s2} - C_{r2} \cot \beta_2 \quad (14)$$

where  $\sigma_{s1}$  and  $\sigma_{s2}$  are the slip factors at

inlet and outlet of impeller.

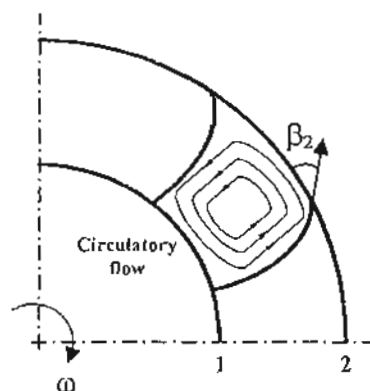
Finally, the circulation head is given as:

$$H_c = [U_2^2 (1 - \sigma_{s2}) + U_1^2 (1 - \sigma_{s1})] / g \quad (15)$$

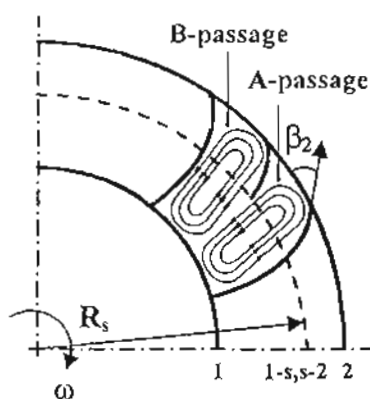
A simplification to the previous equation is suggested assuming no pre-rotation (i.e.  $C_{u1} = 0$  and  $\sigma_{s1} = 1$ ) at the pump flow rate at the design point, then the circulation head is given as:

$$H_c = (1 - \sigma_{s2}) U_2^2 / g \quad (16)$$

The major difficulty in the calculation of the theoretical head in case of using splitters is the correct slip factor to be used.



(a) without splitter



(b) with splitter

Fig. 2 Flow pattern inside the impeller without and with splitter

### 3.4 Inlet Incidence Loss

The inlet incidence loss in impeller is calculated from, Conrad et al. [23]:

$$H_i = f_{inc} \frac{(U_1 - C_{u1})^2}{2g} \quad (17)$$

where  $f_{inc} = 0.5-0.7$ .

### 3.5 Impeller Frictional Head Loss

#### 3.5.1 Impeller Frictional Head Loss in Conventional Case "without Splitter Blades"

The friction head loss in impeller is estimated by the theory of flow between parallel plates and is given by, Gülich [22]:

$$H_f = 4C_d \frac{L_b}{D_h} \frac{W_{av}^2}{2g} \quad (18)$$

where  $C_d$  is the dissipation coefficient,  $D_h$  the hydraulic diameter and  $W_{av}$  the average relative velocity.

The average hydraulic diameter and the average relative velocity are given respectively as, Gülich [22]:

$$D_h = \frac{2(a_2 b_2 + a_1 b_1)}{a_1 + b_1 + a_2 + b_2} \quad (19)$$

$$W_{av} = \frac{2Q}{Z(a_2 b_2 + a_1 b_1)} \quad (20)$$

where,

$$a_1 = \pi D_1 \sin \beta_1 / Z - t \quad (21)$$

$$a_2 = \pi D_2 \sin \beta_2 / Z - t \quad (22)$$

The average impeller Reynolds number is calculated as:

$$Re = \frac{W_{av} L_b}{\nu} \quad (23)$$

The friction coefficient  $C_f$  which corresponds to a flat plate in parallel flow and is function of the Reynolds number

and the roughness  $\varepsilon$ , Gülich [22]:

$$C_f = \frac{0.136}{\left\{ -\log \left( 0.2 \frac{\varepsilon}{L_b} + \frac{12.5}{Re} \right) \right\}^{2.15}} \quad (24)$$

The dissipation coefficient is given as, Gülich [22]:

$$C_d = (C_f + 0.0015)(1.1 + 4b_2/D_2) \quad (25)$$

#### 3.5.2 Impeller Frictional Head Loss in Case of "with Splitter Blades"

The total friction head loss in impeller is estimated as the sum of friction head losses in the sections 1-s and s-2:

$$\begin{aligned} H_{f1} &= H_{f1-s} + H_{fs-2} \\ &= 4C_{d1-s} \frac{L_b - L_s}{D_{h1-s}} \frac{W_{av1-s}^2}{2g} \\ &\quad + 4C_{ds-2} \frac{L_s}{D_{hs-2}} \frac{W_{avs-2}^2}{2g} \end{aligned} \quad (26)$$

where subscripts 1-s refers to the channel from 1 (inlet) to s (leading edge of splitter) and s-2 to the splitter blade leading edge to the impeller exit. The head losses in each of the two split passages of the splitter blade, i.e. A-passage and B-passage, Fig. 2(b), are equal because the splitter is at the middle of the two blades. Also, the hydraulic diameters of these two parallel channels are equal. The hydraulic diameters and the average relative velocities are given respectively as:

$$D_{h1-s} = \frac{2(a_{1-s} b_s + a_1 b_1)}{a_1 + b_1 + a_{1-s} + b_s} \quad (27)$$

$$D_{hs-2} = \frac{2(a_2 b_2 + a_{s-2} b_s)}{a_{s-2} + b_s + a_2 + b_2} \quad (28)$$

$$W_{av1-s} = \frac{2Q}{Z_1(a_{1-s} b_s + a_1 b_1)} \quad (29)$$

$$W_{avs-2} = \frac{2Q}{Z_2(a_2 b_2 + a_{s-2} b_s)} \quad (30)$$



where,

$$a_1 = \pi D_1 \sin \beta_1 / Z_1 - t \quad (31)$$

$$a_{1-s} = \pi D_s \sin \beta_s / Z_1 - t \quad (32)$$

$$a_{s-2} = \pi D_s \sin \beta_s / Z_2 - t \quad (33)$$

$$a_2 = \pi D_2 \sin \beta_2 / Z_2 - t \quad (34)$$

in which  $Z_1$  and  $Z_2$  are the number of blades at the first and second sections, respectively ( $Z_2 = 2Z_1$ ). At the leading edge of splitter blade, the diameter is  $D_s$  and the assumptions of linear decrease of the blade width and the blade angle with the radius are used for the calculations of blade width  $b_s$  and blade angle  $\beta_s$  at the splitter blade leading edge radius.

The dissipation coefficients are calculated similar to the previous procedure taking into consideration the two sections:

$$C_{d1-s} = (C_{f1-s} + 0.0015)(1.1 + 4b_s/D_s) \quad (35)$$

$$C_{ds-2} = (C_{fs-2} + 0.0015)(1.1 + 4b_s/D_2) \quad (36)$$

where,

$$C_{f1-s} = \frac{0.136}{\left\{ -\log \left( 0.2 \frac{\varepsilon}{L_h - L_s} + \frac{12.5}{\text{Re}_{1-s}} \right) \right\}^{2.15}} \quad (37)$$

$$C_{fs-2} = \frac{0.136}{\left\{ -\log \left( 0.2 \frac{\varepsilon}{L_s} + \frac{12.5}{\text{Re}_{s-2}} \right) \right\}^{2.15}} \quad (38)$$

with,

$$\text{Re}_{1-s} = \frac{W_{ov1-s} (L_b - L_s)}{\nu} \quad (39)$$

$$\text{Re}_{s-2} = \frac{W_{ovs-2} L_s}{\nu} \quad (40)$$

### 3.6 Diffusion Loss

The separation may appear in the

impeller at any point. According to Tuzon [13], if the ratio of the relative velocity at the inlet  $W_1$  and the outlet  $W_2$  exceeds a value of 1.4, a portion of the velocity head difference is lost:

$$H_d = 0.25 \left[ \left( \frac{W_1}{W_2} \right)^2 - 2 \right] \frac{W_2^2}{2g} \quad (41)$$

if  $W_1/W_2 > 1.4$ .

### 3.7 Volute Head Loss

The volute head loss results from a mismatch of the velocity leaving the impeller and the velocity in the volute throat. If the velocity approaching the volute throat  $C_3$  is larger than the velocity at the throat  $C_{Q3}$ , the velocity head difference is lost. It is given as, Tuzson [13]:

$$H_{vol} = 0.8 \frac{C_3^2 - C_{Q3}^2}{2g} \quad (42)$$

The velocity approaching the volute throat is calculated from  $C_3 = C_{v2} D_2 / D_3$  where  $D_3$  is the volute throat mean inlet diameter.  $C_{Q3}$  is calculated from the flow rate and the volute throat cross-sectional area.

### 3.8 Disk Friction Loss

The disk friction coefficient is calculated from, Poulikkas [24]:

$$C_M = \left( \frac{k_s}{0.5D_2} \right)^{0.25} \left( \frac{s}{0.5D_2} \right) \text{Re}^{-0.2} \quad (43)$$

in which  $k_s$  is the disk surface roughness,  $s$  the axial gap,  $\text{Re}$  the Reynolds number defined as:

$$\text{Re} = \frac{U_2 (0.5D_2)}{\nu} \quad (44)$$

The frictional torque acting on a rotating radial disk and the disk friction power are

given respectively by:

$$M_{DF} = 0.5 C_M \rho \omega^2 (0.5 D_2)^5 \quad (45)$$

$$P_{DF} = \omega M_{DF} \quad (46)$$

Therefore, the head loss due to the disk friction is calculated from:

$$H_{Disk} = 0.5 C_M \frac{\rho \omega^3 (0.5 D_2)^5}{\gamma Q} \quad (47)$$

### 3.9 Inlet Recirculation Loss

The appearance of inlet recirculation results in a parasitic power demand. Impellers with relatively large inlet diameters; usually encountered in high specific pumps; are the most likely to recirculate. The head loss due to recirculation is given as, Tuzson [25]:

$$H_{Rec} = 0.005 \frac{\omega^3 D_1^2}{\gamma Q} \left(1 - \frac{Q}{Q_o}\right)^{2.5} \quad (48)$$

where  $Q_o$  is the design flow rate. The recirculation loss coefficient depends on the piping configuration upstream of the pump in addition to the geometrical details of the inlet. A default value of 0.005 for the loss coefficient is taken.

### 3.10 Leakage Loss

The leakage flow rate across the front wear ring clearance is calculated from, Tuzson [13]:

$$Q_L = 0.8 (\pi D_1 b_{cf}) \left( H_{thn} - \frac{U_2^2}{8g} \right)^{2.5} \quad (49)$$

The clearance width  $b_{cf}$  is taken as 0.125 mm.

### 3.11 Pump Head

The actual head developed by the pump at any discharge rate is given by, Tuzson [13]:

$$H_m = H_{th} - H_C - H_I - H_f - H_d - H_{vol} \quad (50)$$

### 3.12 Pump Input Power

The input power to the pump is determined using, Tuzson [13]:

$$P_e = \gamma Q (H_{thn} + H_{Disk} + H_{Rec}) \quad (51)$$

### 3.13 Pump Overall Efficiency

The overall efficiency of pump is computed by the following equation, Tuzson [13]:

$$\eta = \frac{H_m}{H_{thn} + H_{Disk} + H_{Rec}} \cdot \frac{Q}{Q + Q_L} \quad (52)$$

## 4. MODIFICATIONS FOR SPLITTER ANALYSIS

### 4.1 Theoretical and Net Theoretical Heads for Centrifugal Impellers with Splitter Blades

The theoretical head delivered to the fluid in centrifugal pumps (Euler turbomachine equation), Eq. (4), decreases very slightly with increasing the number of blades, Fig. 3. The figure shows its variation for number of blades  $Z = 3, 4, 5$  and 6. Also, the theoretical head calculated for an impeller with 3 blades and 3 splitters is plotted, i.e. 3 blades at inlet section and 6 at outlet or simply written  $Z = 3,6$ . The radial velocity at inlet is calculated for a number of blades of 3, while a number of blades of 6 is used for the calculation of the radial velocity at outlet.

The net theoretical head for different numbers of blades  $Z = 3-6$  is illustrated in Fig. 4. The Wiesner slip factor is used in these predictions with  $\beta_2 = 15^\circ$ . The figure also depicts the net theoretical head for an impeller with splitters ( $Z = 3,6$ ).

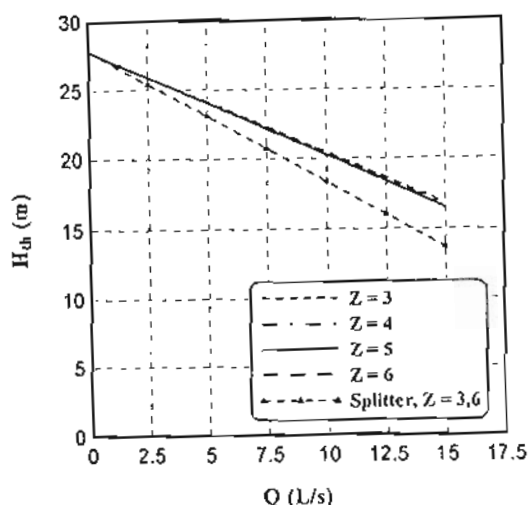


Fig. 3 Variation of  $H_{th}$  with pump discharge for different numbers of blades

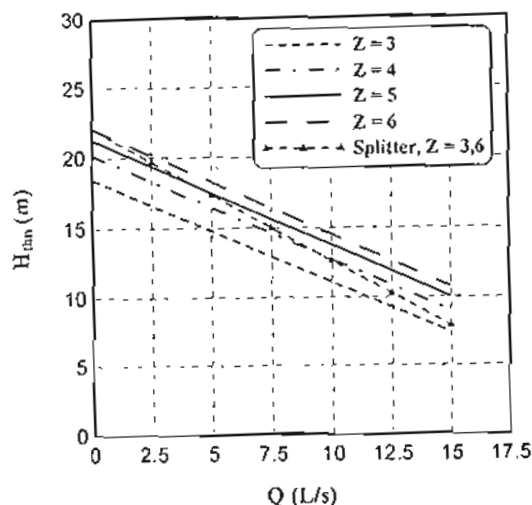


Fig. 4 Variation of  $H_{min}$  with pump discharge for different numbers of blades

Figures 3 and 4 show the physically unsuitable results of the theoretical and net theoretical heads for the splitter case. Adding splitters for an impeller with 3 blades should not decrease the theoretical head than that for 6 blades. Similarly, the net theoretical head for the case ( $Z=3,6$ ) reveals an incorrectness in application of the number of blades in that equations. An appropriate average number of blades should be substituted for  $Z$  in Wiesner slip factor and the radial velocity as discussed in the following section.

#### 4.2 Derivation of Slip Factor for Centrifugal Impellers with Splitter Blades

The slip factors given by many researchers are for impellers with blades only. The utilization of splitter blades within these impellers complicates the study and raises the question of suitability of using the slip factors for the calculation of theoretical head and identification of pump performance curves. Also, most of the slip factors given by researchers are suitable for centrifugal impellers with blades of logarithmic spiral type ( $\beta_1 = \beta_2$ ). The slip factor formulae in general are

function of the number of blades, blade angle and in some formulae on the blade radius ratio ( $R_1/R_2$ ). For other types of blades other than logarithmic spiral, these formulae could be unsuitable. To overcome this problem, a simple method for the prediction of slip factor in case of splitter blades is proposed based on the solidity. The solidity is the blade length,  $L_b$ , divided by spacing at impeller exit:

$$\sigma = \frac{L_b}{2\pi R_2/Z} = \frac{L_b Z}{2\pi R_2} \quad (53)$$

If splitter blades are used, the numerator of Eq. (52) is replaced by the implied sum of the arc lengths of all the blades in the impeller, Karassik et al. [25]. Therefore, the solidity in cases of blades and splitter blades is given as:

$$\sigma = \frac{Z(L_b + L_s)}{2\pi R_2} \quad (54)$$

where  $L_s$  is measured from the outlet diameter of impeller,  $L_s = L_b (D_2 - D_s)/(D_2 - D_1)$ . It is important mentioning that the number of blades  $Z$  remains as in Eq. (53).

The slip factor is defined as, Von

Backström [20]:

$$\sigma_s = 1 - \frac{1}{1 + \sigma F} \quad (55)$$

where  $F$  is the solidity influence coefficient. It is dependent on  $Z$ ,  $\beta_2$  and  $R_1/R_2$ , Von Backström [20]. According to the experimental data given by Buscman [15], Von Backström [20] gave it as:  $F = F_o (\sin \beta_2)^{0.5}$  with  $F_o = 5$ . However, the coefficient  $F$  may differ for each family of impellers.

The simple formula of slip factor proposed by Wiesner [19] can be used to facilitate the computation as:

$$\sigma_s = 1 - \frac{1}{1 + \sigma F} = 1 - \frac{\sqrt{\sin \beta_2}}{Z^{0.7}} \quad (56)$$

thus,

$$F = -\frac{1}{\sigma} \left( 1 - \frac{Z^{0.7}}{\sqrt{\sin \beta_2}} \right) \quad (57)$$

For the blade angle  $\beta_2 = 15^\circ$  and different values of  $Z$ , the following linear relationship and goodness of fit  $R^2$  parameter is deduced between  $F$  and solidity:

$$F = -1.0014\sigma + 6.5818 \quad (R^2 = 0.9985) \quad (58)$$

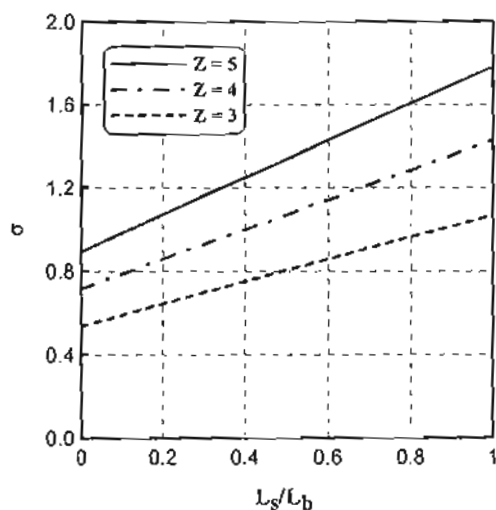


Fig. 5 Variation of solidity with splitter-blade lengths ratio for different numbers of blades

and the slip factor is presented finally for the blade angle  $\beta_2 = 15^\circ$  as:

$$\sigma_s = 1 - \frac{1}{1 + \sigma(-1.0014\sigma + 6.5818)} \quad (59)$$

where the solidity is calculated by Eq. (54). Eq. (59) is used for the prediction of the slip factor in case of impellers with splitter blades. Figures 5 and 6 show the variation of solidity; Eq. (54); and slip factor; Eq. (59); respectively, with splitter-blade lengths ratio  $L_s/L_b$  for different number of blades. For number of blades  $Z = 3$ , Fig. 7 illustrates the slip factor and virtual number of blades corresponding to the existence of splitters with the splitter-blade lengths ratio calculated from:

$$Z_v = \left( \frac{\sqrt{\sin \beta_2}}{1 - \sigma_s} \right)^{1/0.7} \quad (60)$$

The virtual number of blades,  $Z_v$ , in Fig. 7 substitutes the number of blades in the Wiesner slip factor, Eq. (1), and radial velocities, Eqs. (7) and (8) in the case of existence of splitter blades. In the absence of splitter blades, all these equations reduce to the equations for the situation with no splitter blades.

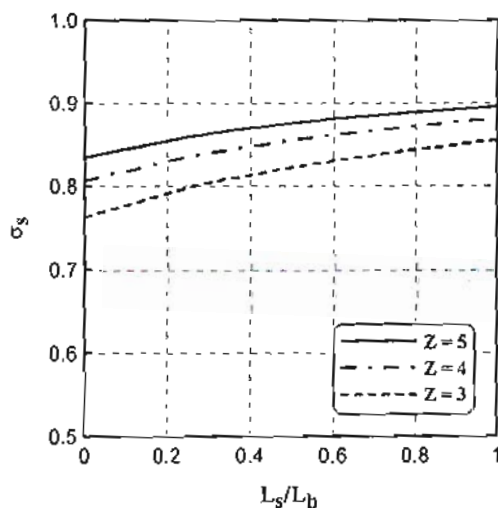


Fig. 6 Variation of slip factor with splitter-blade lengths ratio for different numbers of blades

Table 1 Key parameters of the centrifugal pump, Gölcü et al. [8-10]

Pump speed, $N$ (rpm)	2850
Design flow rate, $Q_o$ (L/s)	10
Design head, $H_m$ (m)	13
Impeller inlet diameter, $D_1$ (m)	0.072
Impeller outlet diameter, $D_2$ (m)	0.132
Inlet blade angle, $\beta_1$ ( $^\circ$ )	18
Outlet blade angle, $\beta_2$ ( $^\circ$ )	15
Blade inlet width, $b_1$ (m)	0.025
Blade outlet width, $b_2$ (m)	0.014
Blade thickness, $t$ (m)	0.004
Blade length, $L_b$ (m)	0.074
No. of impeller blades, $Z$	3, 4, 5, 6, 7
Splitter blade to blade lengths ratio, $L_s/L_b$	0.25, 0.35, 0.5, 0.6, 0.8
Axial gap between disk and housing, $s$ (m)	0.010
Density of water, $\rho$ ( $\text{kg/m}^3$ )	998
Kinematic viscosity of water, $\nu$ ( $\text{m}^2/\text{s}$ )	$1.06 \times 10^{-6}$

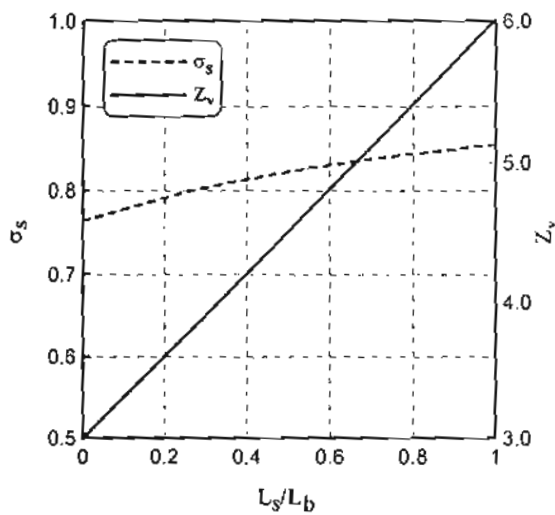


Fig. 7 Variation of slip factor and virtual number of blades with splitter-blade lengths ratio,  $Z = 3$

### 5. CASE STUDY

Gölcü et al. [8-10] used a single-stage centrifugal pump as a deep well pump. Impellers having a different number of blades ( $Z = 3, 4, 5, 6,$  and  $7$ ) with and without splitter blades (25, 35, 50, 60, and 80% of the main blade length) were tested in a deep well pump. The effects of the main blade number and lengths of splitter blades on the pump performance were

investigated. While the number of main blades and the lengths of the splitter blades of a principal impeller were changed, the other parameters such as pump casing, blade inlet and outlet angles, blade thickness, impeller inlet and outlet diameters, were kept the same.

The dimensions of the principal impeller are shown in Fig. 8 and Table 1.

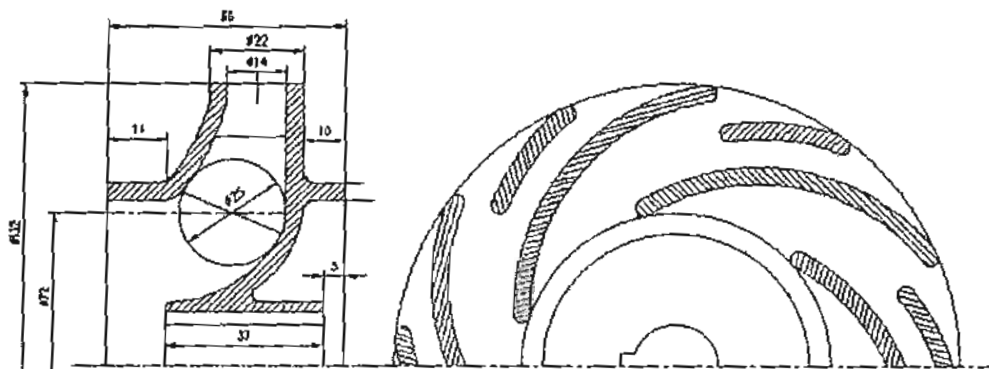


Fig. 8 The dimensions of the principal impeller, Gölcü et al. [10]

## 6. RESULTS AND DISCUSSION

The proposed method is used to estimate the performance of centrifugal pump without splitter blades and with splitter blades. A comparison of the predicted and measured values is presented in the following sections.

The dimensions of the volute were not mentioned in Gölcü et al. [10], therefore using the procedure of volute design, the throat area and the diameter of throat were assumed as  $0.0038 \text{ m}^2$  and  $0.23 \text{ m}$ , respectively. The disk surface roughness  $k_s$  was taken as  $0.003 \text{ m}$ . The coefficient of inlet incidence loss  $f_{inc}$  was proposed 0.7.

The calculations were done using a FORTRAN program which includes the main dimensions, empirical loss models and performance predictions.

### 6.1 Characteristics of the Impellers without Splitter Blades

The effects of the number of impeller blades on deep well pump performance,  $H_m = f(Q)$ ,  $P_e = f(Q)$  and  $\eta = f(Q)$ , investigated experimentally in Gölcü et al. [8-10] using five different impellers with 3, 4, 5, 6, and 7 are shown in Fig. 6(A). It is worth noting that the optimum number of blades determined using the empirical equations was six, Gölcü et al. [8]. A larger number of impeller blades tends to increase the pump generated head (Fig. 9(A)(a)). The head drops rapidly with flow rate for impellers with 3 and 4 blades. However, when  $Z$  is 5, the head decreases gradually without drooping. Impellers with 6 and 7 blades also show similar trends to that with 5 blades.

Figure 9(A)(b) shows the variation of the power as a function of blade number. The power increases proportionally with  $Z$ . The power variation around the design flow rate ( $10 \text{ L/s}$ ) becomes flatter. The maximum power is reached using an impeller with 7 blades.

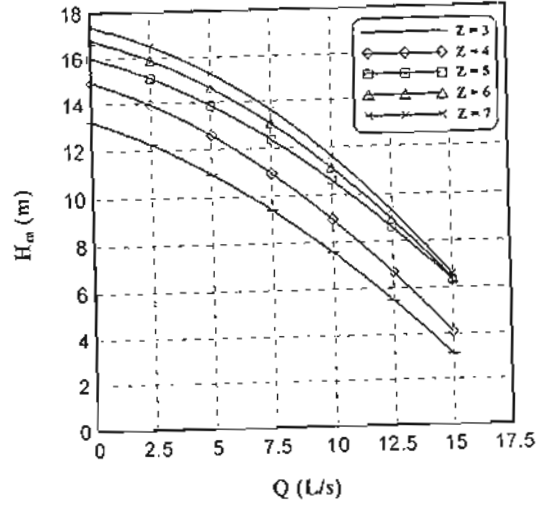
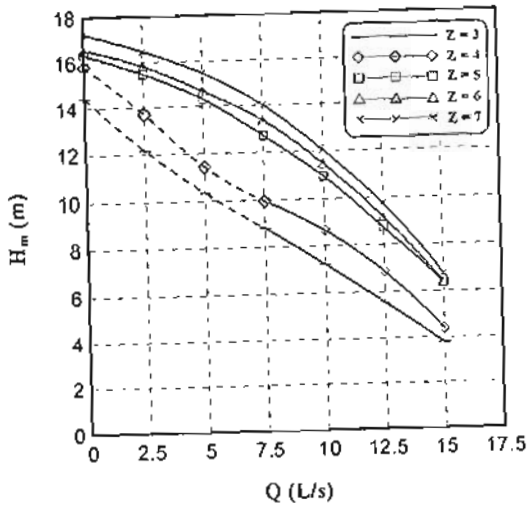
As shown in Fig. 9(A)(c), increasing the number of blades increases the efficiency. At the best efficiency point (BEP), when  $Z = 5$  the efficiency is  $58.36\%$  and the change of efficiency between 5, 6 and 7 blades impellers is very small. Although the impeller with 5 blades has slightly lower efficiency than that with 7, the power consumption of the impeller with 5 blades is approximately  $6.15\%$  less than that of the impeller with 7 blades.

The predicted characteristics of the pump are illustrated in Fig. 9(B). The comparison between calculated and experimental heads, Fig. 9(B)(a), indicates some deviations for impellers with number of blades equal 3 and 4. This is attributed to the difference of number of blades from the optimum number of blades ( $Z = 6$ ) which increases the losses and decreases the guidance of flow through the impeller. For impellers with a number of blades of 5, 6 and 7, there is a better agreement. Figure 10 represents the deviations of predicted values of head and those measured. These deviations are in the range from  $+10$  per cent to  $-16$  per cent, the high negative deviations are at  $Z = 3$ .

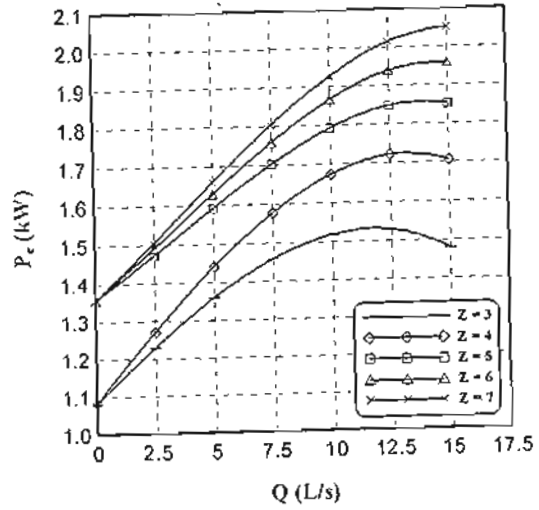
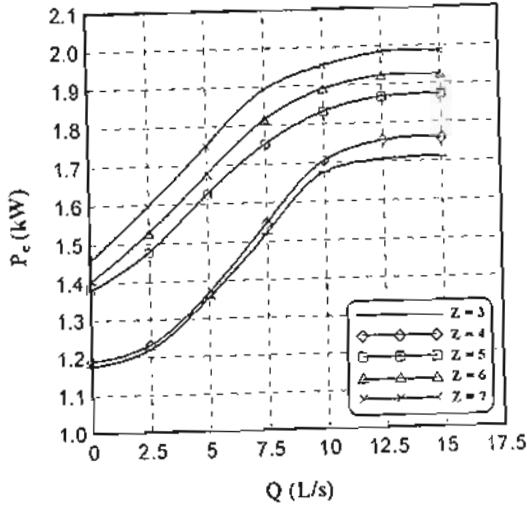
The experimental and predicted input power comparison reveals the steep gradient in the theoretical results till design flow rate ( $10 \text{ L/s}$ ), Fig. 9(B)(b). The maximum and minimum deviations are within  $+6$  per cent and  $-14$  per cent, the latter is at  $Z = 3$ .

The comparison of the predicted overall efficiency of pump, Fig. 9(B)(c), with the corresponding experimental results shows good agreement for impellers with number of blades greater than 3 with maximum and minimum deviations of within  $+8$  per cent and  $-6$  per cent. With  $Z = 3$ , the maximum deviation increases to  $+18$  per cent and at the best efficiency point, the difference in efficiency reaches about  $7\%$ . This is expected as the efficiency is calculated from the pump head and input power and the latter is not well predicted at  $Z = 3$ .

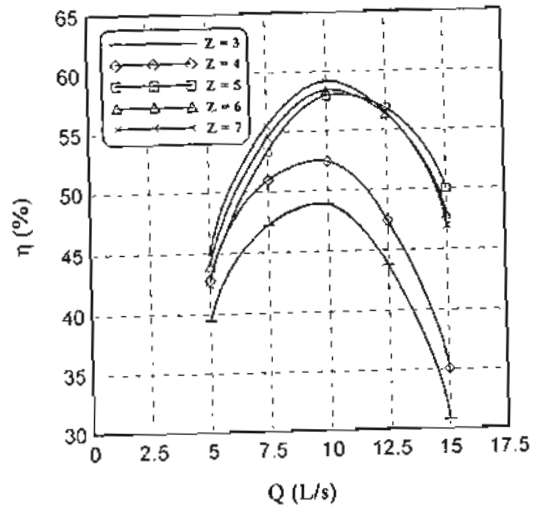
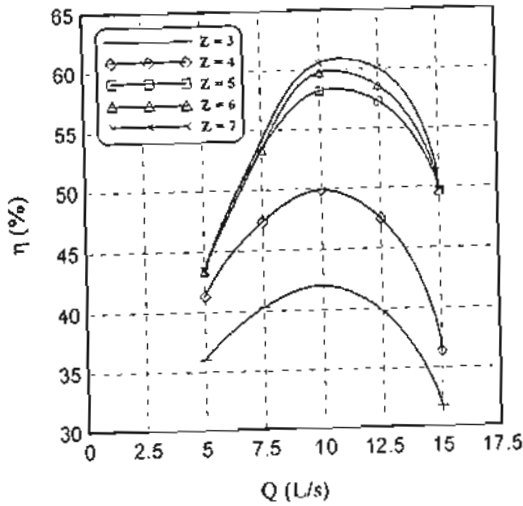
(a)  $H_m$ - $Q$



(b)  $P_c$ - $Q$



(c)  $\eta$ - $Q$



(A) Experimental, Gölcü et al. [10]

(B) Theoretical

Fig. 9 Comparison between experimental and theoretical characteristics for impellers of different number of blades

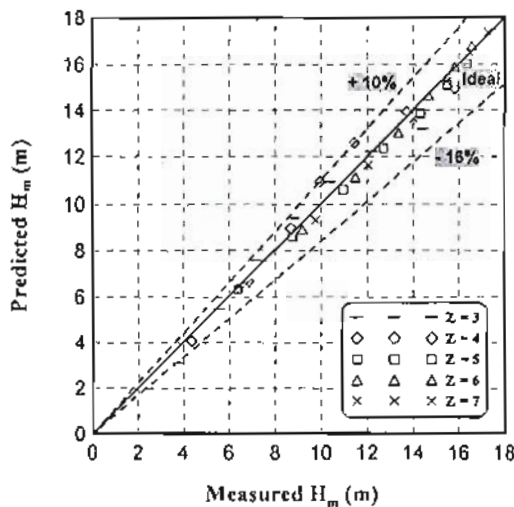


Fig. 10 Comparison between predicted and measured heads for different numbers of blades

## 6.2 Characteristics of the Impellers with Splitter Blades

The effects of different lengths of splitter blades ( $L_s/L_b = 25, 35, 50, 60,$  and  $80\%$ ) were investigated in Gölcü et al. [10] for impellers with 3, 4, 5, 6 and 7 main blades. However, in the present study the two cases of 3 and 4 blades were taken into consideration. For impeller with 5 blades, inserting splitter blades causes a drop in head and shaft power, while the efficiency increases with flow rate up to 10 L/s then it decreases as the splitter blade length increases. For impellers with 6 and 7 blades, the head, power and total efficiency decrease with flow rate as the splitter blade length increases.

### 6.2.1 Characteristics of the Impellers ( $Z=3$ ) with Different Lengths of Splitter Blades

Figure 11(A) shows the experimental pump characteristic curves for the impeller  $Z=3$  with different lengths of splitter blades. The head, input power and overall efficiency increase generally with flow rate as the splitter blade length increases. The rapid drop of the head was improved with the splitter blades  $L_s = 0.6 L_b$  for the

impeller with 3 blades (Fig. 11(A)(a)). Also, as the length of the splitter blade increased, the power consumption increased (Fig. 11(A)(b)). The effect of the splitter blades on efficiency is significant. The splitter blades  $L_s = 0.8 L_b$  result in an increase in the efficiency at the BEP from 42.04% to 56.07% (Fig. 11(A)(c)).

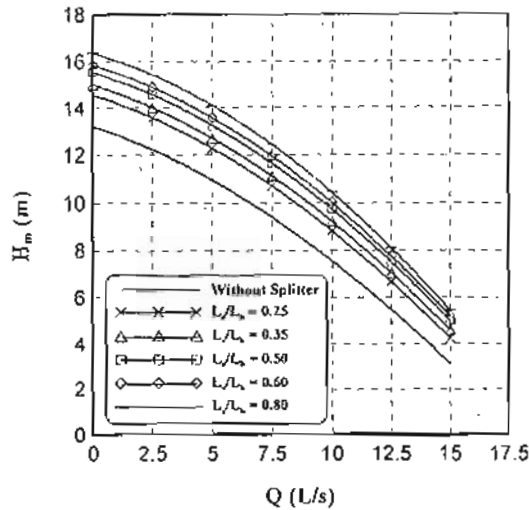
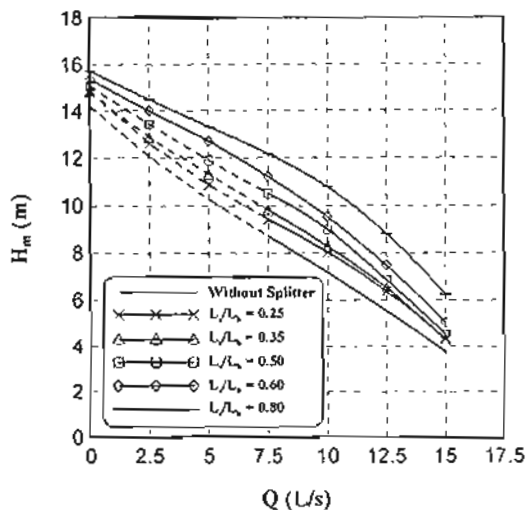
Figure 11(B) shows the theoretical performance curves of the impeller  $Z=3$  with different lengths of splitter blades, where the head, the power, and the pump efficiency are plotted versus the flow rate. The theoretical performance curves, Figure 11(B)(a), show that the effective head has the same trend and in general is in good agreement with the experimental results, except some discrepancies exist especially for the impeller without splitter blades. The deviations are in the range from +13 per cent to -12 per cent, the negative deviations are for  $L_s/L_b = 0.8$ , Fig. 12.

Figure 11(B)(b) illustrates the gradual increase of the theoretical input power with the flow rate till (10 L/s); which is the design flow rate; and a less increase after that. Also, the deviations between the predicted and the experimental results are observed to increase as the shut-off power is approached, which could be due to the underestimation of additional power losses at low discharge rates. The deviations of the theoretical power results for different  $L_s/L_b$  are within +7 per cent and -4 per cent. The theoretical power for impeller without splitter ( $Z=3$ ) is given in Figure 9(B)(b).

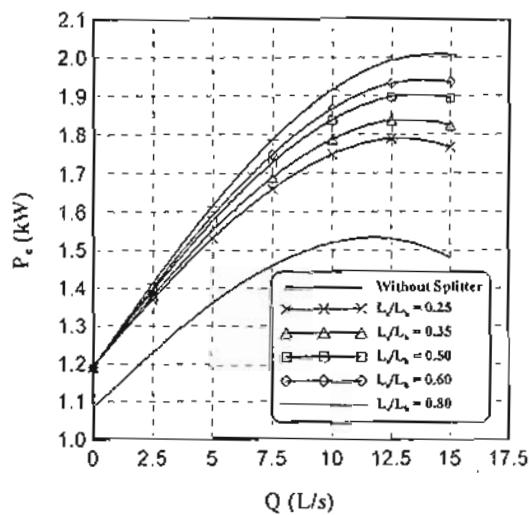
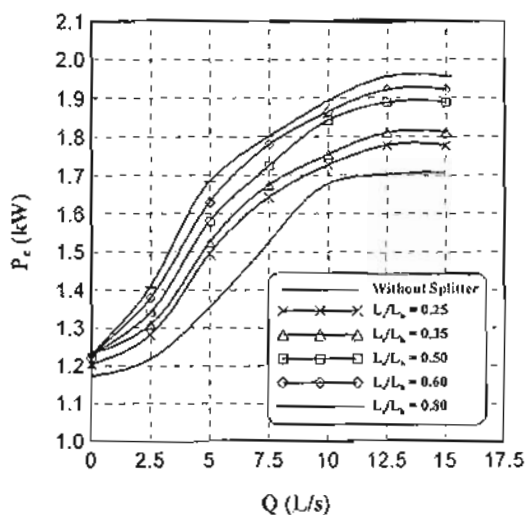
The theoretical pump efficiency, Figure 11(B)(c), is higher than the experimental ones for  $L_s < 0.8 L_b$ . The maximum and minimum deviations of the theoretical efficiency results for different  $L_s/L_b$  are within +13 per cent and -15 per cent. The minimum deviation is for  $L_s/L_b = 0.8$ . These high deviations resulted because the calculated efficiencies are based on the head and the input power.



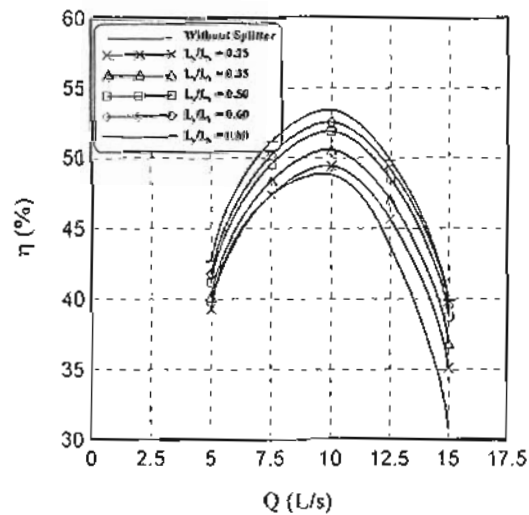
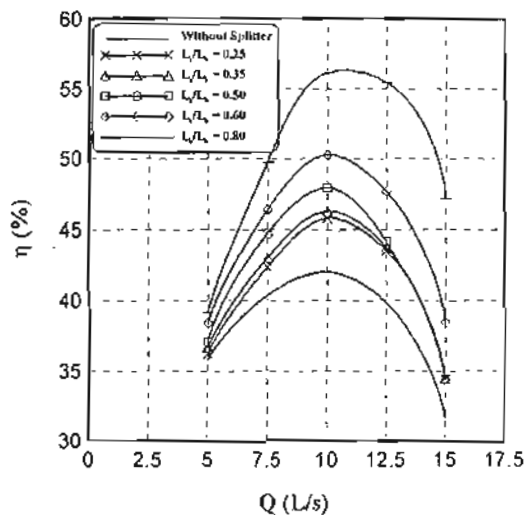
(a)  $H_m$ - $Q$



(b)  $P_c$ - $Q$



(c)  $\eta$ - $Q$



(A) Experimental, Gölcü et al. [10]

(B) Theoretical

Fig. 11 Comparison between experimental and theoretical characteristics of the impeller ( $Z = 3$ ) with different lengths of splitter blades

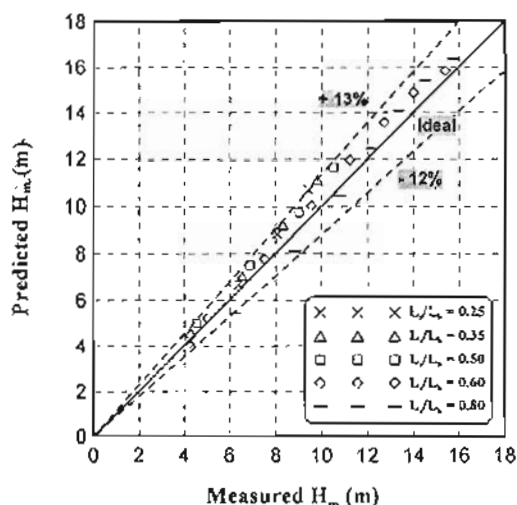


Fig. 12 Comparison between predicted and measured heads of the impeller ( $Z = 3$ ) with different lengths of splitter blades

### 6.2.2 Characteristics of the Impellers ( $Z = 4$ ) with Different Lengths of Splitter Blades

The experimental pump characteristics curves for the impeller  $Z = 4$  with different lengths of splitter blades are shown in Fig. 13(A). As in the experimental results for  $Z = 3$ , the head, power and total efficiency increase generally with flow rate as the splitter blade length increases. The improvement in rapid drop of the head was achieved with the splitter blades  $L_s = 0.5 L_b$ , (Fig. 13(A)(a)). The power consumption increases with the increase of the length of the splitter blade (Fig. 13(A)(b)). For the efficiency, the splitter blades  $L_s = 0.8 L_b$  result in an increase in the efficiency at the best efficiency point from 49.71% to 56.08% (Fig. 13(A)(c)).

Figure 13(B) illustrates the theoretical pump characteristics curves for the impeller  $Z = 4$  with different lengths of splitter blades. For the head versus flow rate, Figure 13(B)(a), it may be seen that there is some discrepancy between the theoretical and experimental results; the

theoretical heads at shut-off are greater than that from experiments for all  $L_s / L_b$ .

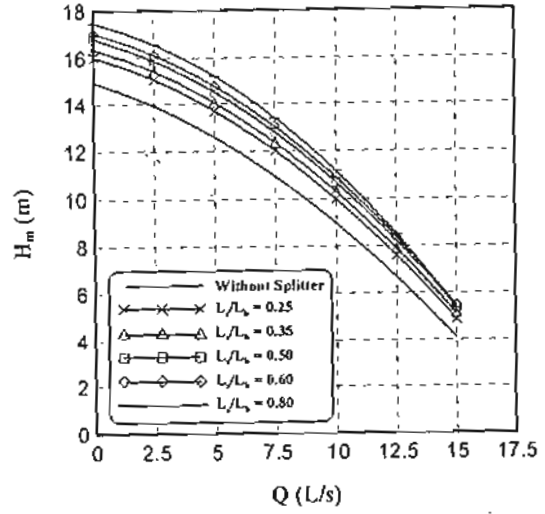
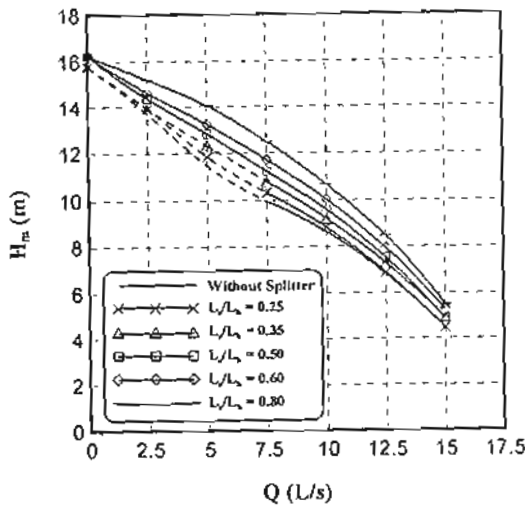
To gain an insight into the applicability of the derived correlation for the slip factor, a comparison is made between the predicted and measured pump heads. Figure 14 depicts the comparison of predicted and measured heads for main blades  $Z = 4$  with different lengths of splitter blades. It is seen that the data points are distributed over the perfect-fit line and the deviations are within +17 per cent. It is to be noted that the predicted values are higher than the measured values and the maximum deviations are at  $L_s / L_b = 0.25$ .

The theoretical input power, Figure 13(B)(b), increases gradually with the flow rate till the design flow rate (10 L/s) with less increase after that. Also, it has low increase at low discharge rates (2.5 – 7.5 L/s) with the increase of lengths of splitter blades compared with the experimental results. This may be attributed to the loss models. The theoretical power for impeller without splitter ( $Z = 4$ ) is given in Figure 9(B)(b). As in the previous cases, the deviations between the predicted and measured input power are within +17 per cent and -1 per cent.

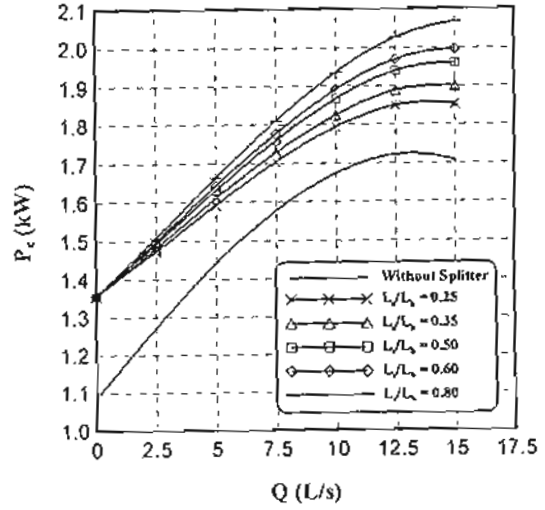
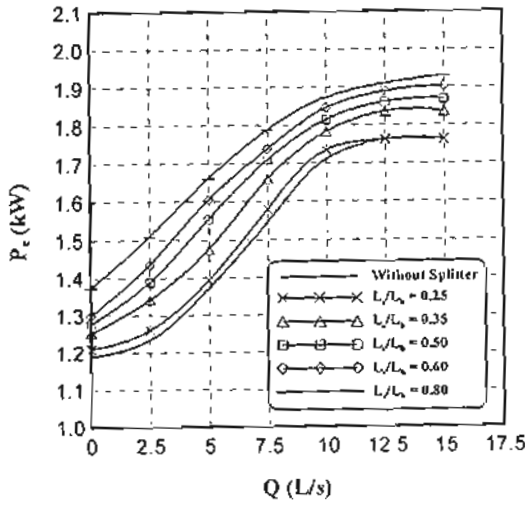
The comparison of the predicted overall efficiency of pump, Fig. 13(B)(c), with the corresponding experimental results shows similar trends at best efficiency point ( $Q = 10$  L/s) and over-prediction at  $L_s / L_b < 0.80$ . At different  $L_s / L_b$ , the maximum and minimum deviations are +10 per cent and -8 per cent, respectively. The minimum deviations corresponds to  $L_s / L_b = 0.80$ .

After analyzing the results obtained from the derived slip factor correlation, it seems that the possible causes of deviations could be minimized if individual effects of derived slip factor and virtual number of blades on the pump head are considered.

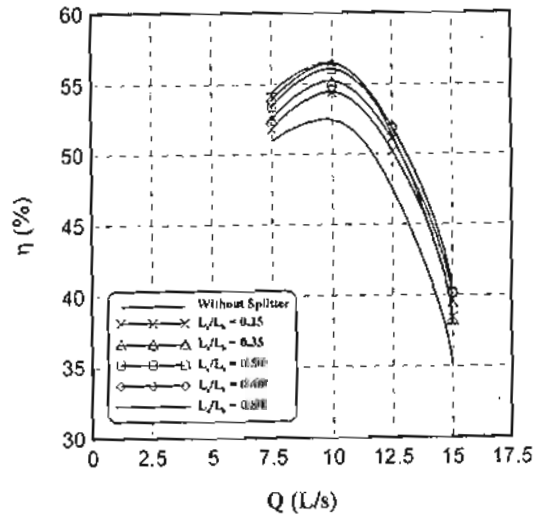
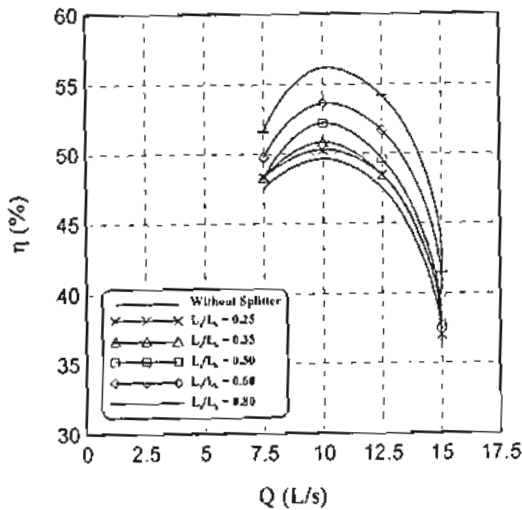
(a)  $H_m$ - $Q$



(b)  $P_c$ - $Q$



(c)  $\eta$ - $Q$



(A) Experimental, Gölcü et al. [10]

(B) Theoretical

Fig. 13 Comparison between experimental and theoretical characteristics of the impeller ( $Z = 4$ ) with different lengths of splitter blades

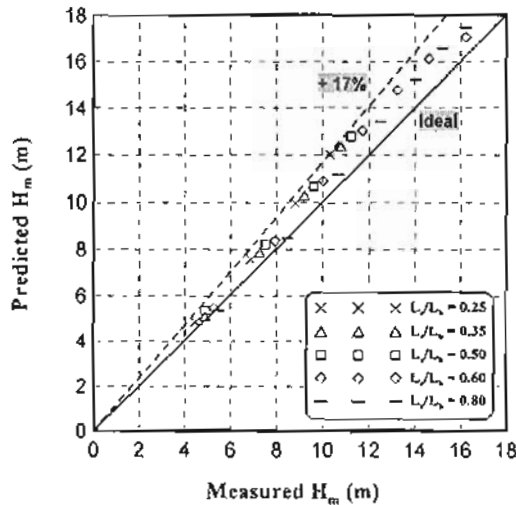


Fig. 14 Comparison between predicted and measured heads of the impeller ( $Z = 4$ ) with different lengths of splitter blades

## 7. CONCLUSIONS AND RECOMMENDATIONS

A simple theoretical approach has been identified to predict the performance of centrifugal impeller equipped with splitter blades. In particular, the present study has focused on the theoretical calculation of head. The slip factor for a centrifugal pump impeller with splitter blades was estimated by means of blade solidity. A methodology is proposed in order to achieve the prediction of performance of centrifugal pumps. The methodology was carried out for impellers with and without splitters. Based on the results, the main obtained conclusions are summarized below:

- (1) An appropriate empirical slip relationship which depends on the solidity is derived for impellers with splitters, Eq. (59).
- (2) The virtual number of blades,  $Z_v$ , which substitutes  $Z$  in the Wiesner slip factor in case of existence of splitter blades is calculated by the suggested approach, Eq. (60).
- (3) The theoretical head is determined using the slip factor and the virtual number of blades. Consequently, all

the relevant flow conditions can be determined at the impeller exit.

- (4) The proposed prediction methodology has proved to improved performance of impellers with splitter blades.
- (5) The consideration of the individual effects of derived slip factor and virtual number of blades on the pump head could minimize the deviations between the predicted and measured pump heads.
- (6) New approaches using computational fluid dynamics (CFD) simulations need to be developed in order to estimate correctly the slip factor and to provide improvements to the performance prediction technique for centrifugal impellers with splitter blades.

## References

- [1] Cui, B., Zhu, Z., Zhang, J., and Chen, Y., "The Flow Simulation and Experimental Study of Low-Specific-Speed High-Speed Complex Centrifugal Impellers," *Chinese Journal of Chemical Engineering*, Vol. 14, No. 4, 2006, pp. 435-441.
- [2] Zuchao, Z., Qingming, J., and Dunhui, H., "Experimental Study on High-Speed Centrifugal Pumps with a Half-Open Complex Impeller," *The Fifth International Conference on Fluid Power Transmission and Control (ICFP 2001)*, Hangzhou, China, April 3-5, 2001.
- [3] Nakase, Y., and Senoo, Y., 1973, "Theoretical Research on the Flow in Impellers," 3rd Report, Flow in Rotating Blade-Rows with Splitter Blades, *Transactions of the Japan Society of Mechanical Engineers, B*, Vol. 39(322).
- [4] Khlopenkov, P.R., "Optimization of Centrifugal Pumps," *Power Technology and Engineering*, Vol.

- 16, No. 10, Oct. 1982, pp. 533-539.
- [5] Gui, L., Gu, C., and Chang, H., "Influences of Splitter Blades on the Centrifugal Fan Performances," *ASME Gas Turbine and Aeroengine Congress and Exposition*, Toronto, 4-8 June, 1989, Paper 89-GT-33.
- [6] Miyamoto, H., Nakashima, Y., and Ohba, H., "Effects of Splitter Blades on the Flows and Characteristics in Centrifugal Impellers," *JSME Int. J.*, Ser. II, Vol. 35, No. 2, 1992, pp. 238-246.
- [7] Yuan, S., "Advances in Hydraulic Design of Centrifugal Pumps," *ASME Fluids Engineering Division Summer Meeting*, Vancouver, British Columbia, Canada, June 22-26, 1997, pp. 1-15.
- [8] Gölcü, M., and Pancar, Y., "Investigation of Performance Characteristics in a Pump Impeller with Low Blade Discharge Angle," *World Pumps*, Issue 468, September 2005, pp. 32-40.
- [9] Gölcü, M., Pancar, Y., and Sekmen, Y., "Energy Saving in a Deep Well Pump with Splitter Blade," *Energy Conversion and Management*, Vol. 47, 2006, pp. 638-651.
- [10] Gölcü, M., Usta, N., and Mancar, Y., "Effects of Splitter Blades on Deep Well Pump Performance," *Journal of Energy Resources Technology*, Vol. 129, Sep. 2007, pp. 169-176.
- [11] Kergourlay, G., Younsi, M., Bakir, F., and Rey, R., "Influence of Splitter Blades on the Flow Field of a Centrifugal Pump: Test-Analysis Comparison," *International Journal of Rotating Machinery*, Vol. 2007, 2007, Article ID 85024, 13 pages.
- [12] Ukhin, B.V., "Effect of the Quantity and Shape of Impeller Blades on Dredge Pump Parameters," *Power Technology and Engineering*, Vol. 36, No. 3, 2002, pp. 168-172.
- [13] Tuzson, J., *Centrifugal Pump Design*, John Wiley & Sons Inc., New York, 2000.
- [14] Zaher, M.A., "Approximate Method for Calculating the Characteristics of a Radial Flow Pump," *Proceedings of the Institution of Mechanical Engineers, Part E, Journal of Process Mechanical Engineering*, Vol. 215, No. 4, 2001, pp. 295-316.
- [15] Busemann, A., "Das Förderhöhenverhältniss Radialer Kreiselpumpen mit Logarithmisch-Spiraligen Schaufeln," *Zeitschrift für Angewandte Mathematik und Mechanik*, Vol. 8, 1928, pp. 371-384.
- [16] Pfleiderer, C., *Die Kreiselpumpen für Flüssigkeiten und Gase*, 5te Auflage, Springer-Verlag, 1961.
- [17] Stodola, A., *Steam and Gas Turbines with a Supplement on the Prospects of the Thermal Prime Mover*, Authorized translation from the Sixth German Edition by Louis C. Loewenstein. Reprinted by Peter Smith, 1945, New York, pp. 1259-1260.
- [18] Stanitz, J.D., "Some Theoretical Aerodynamic Investigations of Impellers in Radial- and Mixed-Flow Centrifugal Compressors," *Transactions of the ASME*, Vol. 74, 1952, pp. 473-476.
- [19] Wiesner, F.J., "A Review of Slip Factors for Centrifugal Impellers," *Trans. ASME, Journal of Engineering for Power*, Vol. 89, 1967, pp. 558-572.
- [20] Von Backström, T.W., "A Unified Correlation for Slip Factor in Centrifugal Impellers," *ASME Journal of Turbomachinery*, Vol. 128, 2006, pp. 1-10.
- [21] Memardefzouli, M., and Nourbakhsh, A., "Experimental Investigation of Slip Factors in Centrifugal Pumps," *Experimental Thermal and Fluid Science*, Vol. 33, 2009, pp. 938-945.
- [22] Gülich, J.F., *Centrifugal Pumps*, Springer-Verlag Berlin Heidelberg, 2008.

- [23] Conrad, O., Raif, K., and Wessels, M., "The Calculation of Performance Maps for Centrifugal Compressors with Vane-Island Diffusers," Proceedings of the ASME 25th Annual International Gas Turbine Conference and 22nd Annual Fluids Engineering Conference on *Performance Prediction of Centrifugal Pumps and Compressors*, New Orleans, Louisiana, March 9-13, 1980, pp. 135-147.
- [24] Poullikkas, A., "Surface Roughness Effects on Induced Flow and Frictional Resistance of Enclosed Rotating Discs," *Trans. ASME, Journal of Fluids Engineering*, Vol. 117, 1995, pp. 526-528.
- [25] Tuzson, J., "Inlet Recirculation in Centrifugal Pumps," *ASME Symposium on Performance Characteristics of Hydraulic Turbines and Pumps*, Winter Annual Meeting, Boston, 1983, FED Vol. 6, pp. 195-200.
- [26] Karassik, I.J., Messina, J.P., Cooper, P., and Heald, C.C., *Pump Handbook*, Fourth Edition, McGraw-Hill Companies, Inc., 2008.